EXPERIMENTAL STUDY ON MECHANICAL BEHAVIOR OF DAMAGE CONTROLLED PRECAST-PRESTRESSED CONCRETE FRAME WITH P/C MILD-PRESS-JOINT

H. Sakata[1], A. Wada[2], Y. Matsuzaki[3], and K. Nakano[4]

1) Associate Professor, Structural Engineering Research Center, Tokyo Institute of Technology, Japan
2) Professor, Structural Engineering Research Center, Tokyo Institute of Technology, Japan
3) Professor, Department of Architecture, Tokyo University of Science, Japan
4) Managing Director, Nakano Building Research & Associate., Japan
hsakataq@serc.titech.ac.jp, wada@serc.titech.ac.jp, ymatsu@rs.kagu.tus.ac.jp

Abstract: This paper presents results of the experiment to certify the mechanical behaviors of the frame structures by precast-prestressed concrete with MILD-PRESS-JOINT. The specimen is cruciform model of prototype frame with MILD-PRESS-JOINT. The beam and column members precast-prestressed concrete are connected by prestressing strand that go through the beam and column, and anchored at the end of beam. Specimens have following parameter, with or without corbel of column and strand arrangement. The following conclusions were drawn from the study where partial frame experiments were conducted using prestressing strands and verification was obtained by comparison with RC frames. 1) The frame using the PC Mild Press Joint has extremely small residual deformation showed high restoration capability. 2) Damage was limited to the part near the beam column interface. Damage could be controlled.

1. INTRODUCTION

1.1 Background and Purpose of Study

In the light of depleting natural energy resources, global environmental issues, etc. there are important issues in future seismic design for rarely occurring large earthquake ground motions. It will be necessary not only to avoid building collapse and to protect human lives, but also to determine post-earthquake building damage, to minimize such damage and to continue using the buildings.

A PC Mild Press Joint [1] has been used to control damage to concrete structures during earthquakes. This joint press binds prestressed concrete columns and beams. It thus controls damage by limiting cracks and utilizing the characteristics of origin-restoration capability, etc. It is expected to be effective in future seismic designs. However, there have been almost no experimental studies on PC Mild Press Joints. Thus, full understanding has not been gained on their mechanical characteristics. The purpose of this study is to clarify the mechanical characteristics of the frames using PC Mild Press Joints.

1.2 Overview of PC Mild Press Joint Method

The columns and beams are assembled with high quality precast and prestressed concrete members ($F_c > 50 N/mm^2$) using the PC Mild Press Joint method. The members are press-bound and integrated using prestressing steel (prestressing strands) for jointing. The prestress force introduced for the press binding is set at 50% of the nominal yield strength of prestressing strand (Py). Conceptual skeleton curves of the frame for prestress forces 0.75Py, 0.5Py and 0.25Py are shown in Figure 1. The PC Mild Press Joint method practices the control by setting the prestress force introduced to prestressing steel at 0.5Py, as shown in Figure 1. Control is attained so as not to cause yield of the prestressing strands, as shown in the 0.75Py case, or excess deformation, as shown in the 0.25Py case, at maximum strength until the targeted story deformation angle (R = 1/75 rad) is reached.

2. EXPERIMENT PROGRAM

2.1 Specimen

The specimen configurations and bar arrangement details are shown in Figure 2. The specimen parameters and material characteristics are shown in Table 1. Specimen Series I were beam yield preceding type. Specimen Series II suffered larger shear force in the joint panel. Both Series I and Series II were of two kinds, i.e. a partial frame using PC Mild Press Joint (hereinafter called PC specimen) and an RC-structured partial frame (hereinafter called RC specimen). Settings for beam shear span-to-depth ratio 3.0 and column shear span-to-depth ratio 2.2 were made common for all the test pieces. In each PC specimen, prestressing strands were placed in two rows on the beam cross-section and the main beam bars (normal reinforcing bars) did not penetrate the joint panel. Series I and II has one RC specimen, respectively. The beam flexural strengths of each of them were made the same as those of the PC specimen in Series I and II. Column flexural strengths of all specimens were made about 1.4 times the beam flexural strength. The ration of shear strength to flexural strength of the beams and column was about 1.7.

2.2 Experiment Method

The loading apparatus and loading cycle are shown in Figure 3. A shear force was applied to the right and left beams using two hydraulic of 490 kN jacks, as shown in Figure 3. The vertical displacements at the loading point were controlled keeping the same when the shear force was applied. Increasing cyclic loading was carried out according to the loading cycle shown in Figure 3. An axial force of about 745 kN (axial force ratio = 0.08 [Fc: 90 N/mm^2], =0.15 [Fc: 50 N/mm^2]) was applied to the column using an unbonded prestressing rod built into the column member.

The Jack load, displacement, strain of the steel member and crack width were measured. The widths of cracks across the
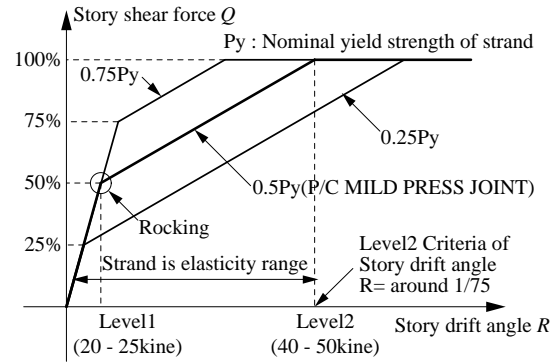

Figure 1 Conceptual Skeleton Curve of The Frame for Various Level of Prestress Forces
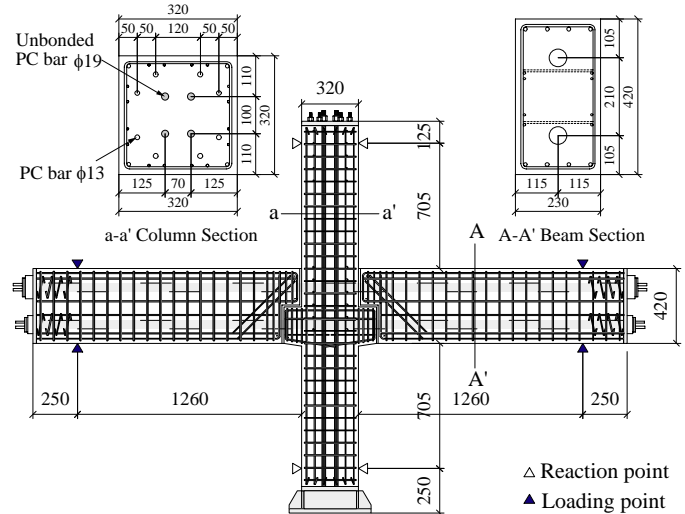

Figure 2 Specimen (PC-42-C-90)

1: Specimen, 2: Pin-roller, 3: Column pin support aparatus, 4: 490kN oil jack, 5: Holder for displacement measurement, 6: PC bar, 7: Load-cell, 8: Lateral deformation restriction channel

$$Q = \frac{Q_L + Q_R}{2} \cdot \frac{L}{H}$$

$$R = \frac{\delta_L + \delta_R}{L}$$

Q_L: Left beam shear force
Q_R: Right beam shear force
δ_L: Vertical displacement at Left-beam loading point
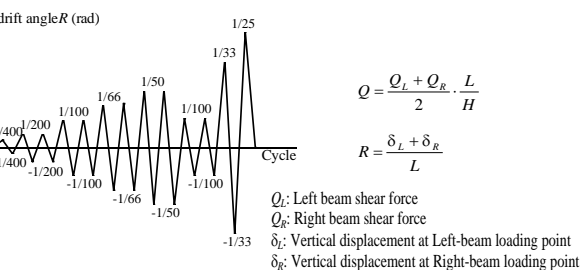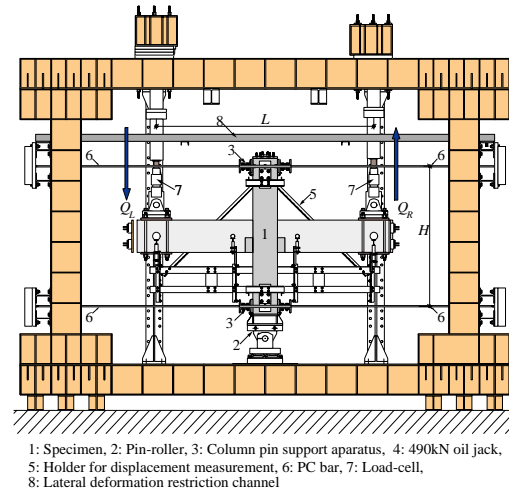δ_R: Vertical displacement at Right-beam loading point

Figure 3 Loading Apparatus and Loading Cycle

shear reinforcing bar where strain gauges were attached were measured for Series II at the time of peak story drift angle using a digital microscope with a minimum scale of 0.01mm.

Table 1   Specimen parameters and material characteristics

Series	Specimen	Number of Strand *1 (Main Reinforcement)		Corbel	$_c\sigma_B$ beam/ column N/mm²	E_c beam/ column kN/mm²	$_c\sigma_t$ beam/ column N/mm²	$_p\sigma_y(_s\sigma_y)$ N/mm²	$E_p(E_s)$ kN/mm²	σ_p N/mm²
		Upper	Lower							
		Number of Strand								
	PC42-C-90	4	2	with	92.0	44.6	4.3	1762	195	4.84
	PC42-N-90	4	2	without	92.4	43.6	3.5			
	PC33-C-90	3	3	with	87.5	43.1	3.3			
	RC33-50	(7-D16 ²)	(7-D16 ²)		58.0	37.0	3.5	(357)	(195)	
	PC55-C-90	5	5	with	91.5	42.5	3.9	1628	212	8.07
	PC55-C-50	5	5	with	86.3/55.8	40.4/35.2	3.8/3.3			
	RC55-50	(7-D16 ³)	(7-D16 ³)		56.8	37.2	3.2	(538)	(193)	

∗1:PC Strand (SWPR7B), *2:SD295A, *3:SD490, $_c\sigma_B$: Concrete Compressive Strength,

E_c: Concrete Young's Modulus, $_c\sigma_t$: Concrete Tensile Strength,

$_p\sigma_y$: Strand Yield Strength (0.2%offset), $_s\sigma_y$: Beam Main Reinforcement Yield Strength,

E_p: Strand Young's Modulus, E_s: Beam Main Reinforcement Young's Modulus

3. EXPERIMENT RESULTS AND DISCUSSIONS

3.1 Characteristics of Failure and Deformation

Figure 4 shows the part in the vicinity of the column/beam joint at the time of maximum deformation. Figure 5 shows the relationship of story shear Q – story drift angle R. Only one of the PC specimens shows whole hysteresis. Envelopes are shown for the other specimens, since the characteristics were almost the same. The Q – R relationship of the PC specimens indicates that their hysteresis characteristics belonged to the origin-oriented type having small residual deformation for both Series I and II. No yielding of the prestressing strands was observed. Damage was only observed near the press joint. Yield of shear reinforcing bars at the joint was observed at $R = 1/66$ rad in PC55-C-50. The RC specimens showed spindle-shaped hysteresis with narrow hysteresis up to $R = 1/66$ rad and slip type restoration characteristics after about $R = 1/50$ rad in RC33-50. Considerable damage occurred at the joint. RC33-50 reached the maximum story shear force at $R = 1/100$ rad and the main reinforcing bar of the beam yielded. The shear reinforcing bar at the joint yielded at the same cycle. For the RC55-50, the shear reinforcing bar of the joint yielded at $R = 1/100$ rad. The main reinforcing bar of the beam yielded at $R = 1/50$ rad. PC55-C-50 was designed so that joint failure preceded others. However, little damage occurred at the joint, because the shear force input to it reached the ceiling due to beam end crushing. Decreasing strength was observed after $R = 1/66$ rad where beam end crushing was observed.

3.2 Conditions of Joint Damage

Figure 6 shows the strain of the shear reinforcing bar used in the joint at peak story drift angle. Figure 7 shows the sum of crack widths at peak story drift angle at the joint. Figure 8 shows the sum of widths of residual cracks. As crack widths in the joint increased, strain of shear reinforcing bars of the joint increased. The crack widths of PC55-C-50 and RC55-50 were compared. In PC55-C-50, the shear reinforcing bars of the joint reached yield. The sum of crack widths at the peak was about 10 times larger in RC55-50 than in PC55-C-50. Meanwhile, the sum of widths of residual cracks during unloading was about 25 times larger in RC55-50. This indicates that more cracks closed in PC55-C-50 than in RC55-50 during unloading.
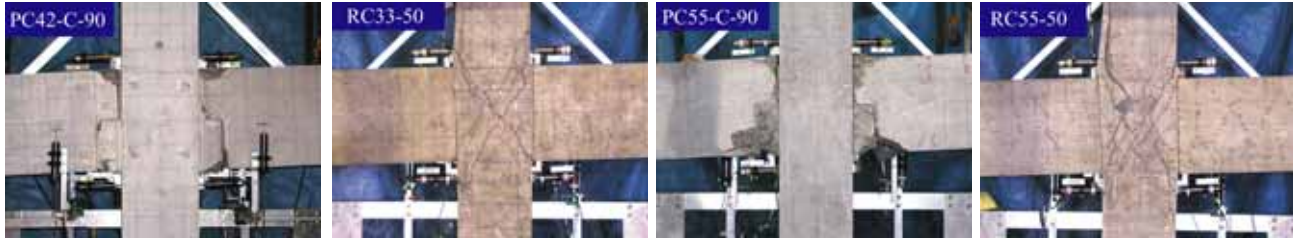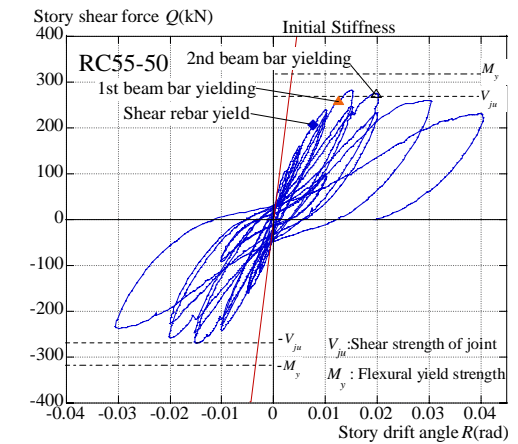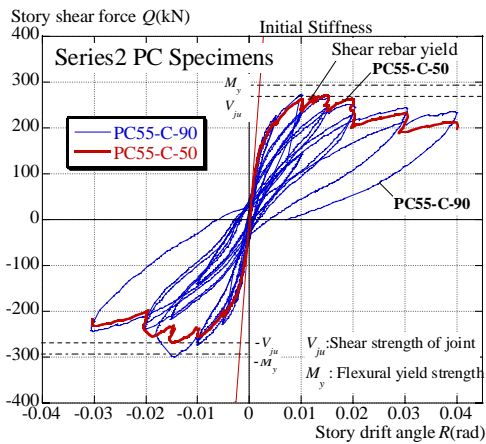
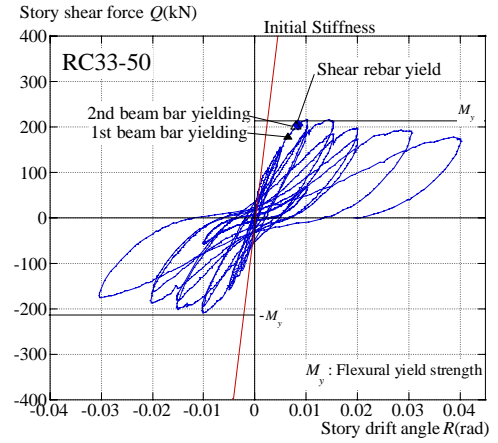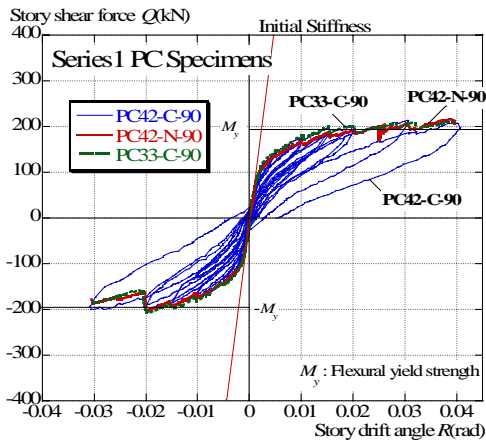Figure 4   Ultimate Stage (R=1/25rad)

Figure 5   Story Shear Force Q – Story Drift Angle R Relationships
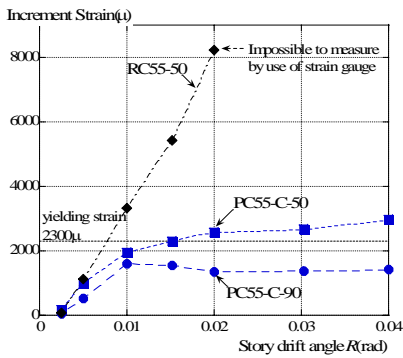

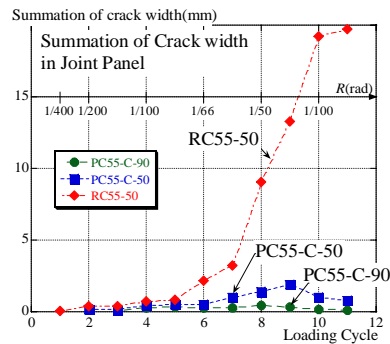Figure 6   Strain of Shear Reinforcement in Joint Panel

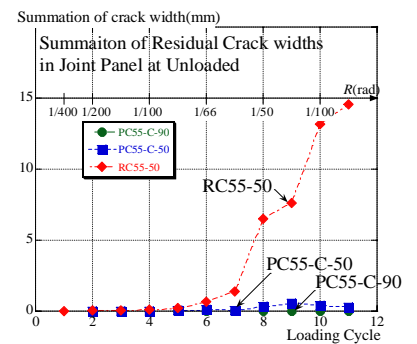Figure 7   Summation of Crack Width at Peak Point of Each Cycle

Figure 8   Summation of Residual Crack Width

3.3 Studies on Strength of Joint

To study the strength of the joint, the shear crack strength $_{ex}\tau_{cr}$ of the joint during the experiments was first estimated. $_{ex}\tau_{cr}$ was obtained from Equation (1). V_{jcr} is the shear force input to the joint when the crack first occurs at the joint, as obtained from Equation (2). The tensile force was obtained from Equation (3). The shear crack strength of the joint of the RC specimen was obtained from Equation (4).

$$_{ex}\tau_{cr} = \frac{V_{jcr}}{b_j D_j} \tag{1}$$

$$V_{jcr} = 2T - V_c \tag{2}$$

$$_{RC}\tau_{cr} = \sqrt{f_t^2 - \sigma_0 f_t} \tag{3}$$

$$T = \frac{M_b}{j} = \frac{Q_b \cdot a}{j} \tag{4}$$

where [b_j: Effective joint width, D_j: Column height, T: Tensile force of prestressing steel or tensile force of normal reinforcing bar, V_c: Column shear force (story shear force), M_b: Moment of beam end, Q_b: Beam shear force, a: Shear span, j: Distance between tension and compression resultants (= 7/8 d, d: Effective depth), f_t: Tensile strength of concrete, σ_0: Column axial stress]

$_{ex}\tau_{cr}$ obtained from Equation (1) and $_{RC}\tau_{cr}$ obtained from Equation (4) are shown with solid lines in Figure 9. $_{ex}\tau_{cr}$ and Equation (4) were compared. RC33-50 ( ) and RC55-50( ) showed general matching with Equation (4). However, $_{ex}\tau_{cr}$ of all PC specimens became larger than that from Equation (4). Shear crack strength in the PC specimens was evaluated using $_{PC}\tau_{cr}$, showing that the shear crack strength incorporated the beam prestress. $_{PC}\tau_{cr}$ was obtained from Equation (5).

$$_{PC}\tau_{cr} = \sqrt{f_t^2 - (\sigma_0' + \sigma_p) \cdot f_t + \sigma_0' \cdot \sigma_p} \tag{5}$$

[f_t: Tensile strength of concrete, σ_0': Axial stress of column taking into account the column prestress, σ_p: Stress due to beam prestress (Series I: $\sigma_p = 4.02\text{N/mm}^2$, Series II: $\sigma_p = 7.61\text{N/mm}^2$)]
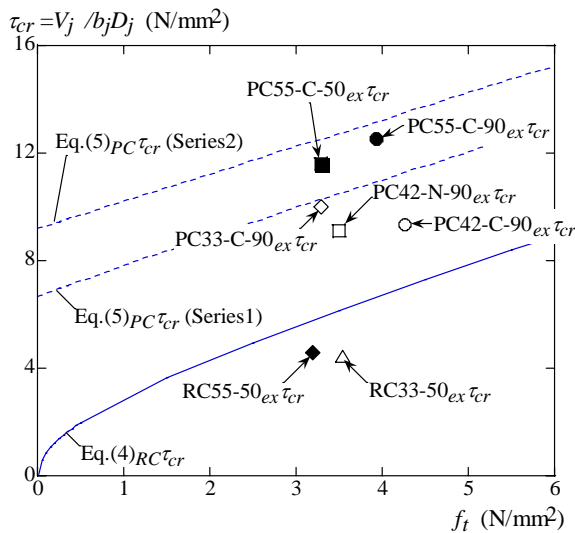

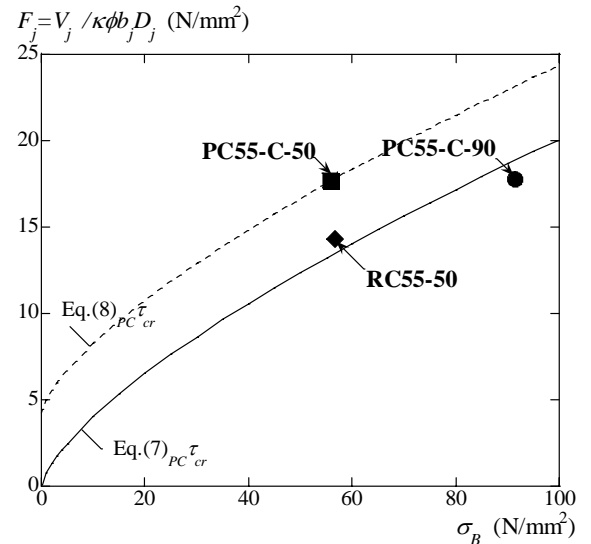Figure 9   Shear Crack Strength

Figure 10   Shear Strength

Shear crack strength $_{PC}\tau_{cr}$ calculated from Equation (5) is shown with a dashed line in Figure 9. $_{ex}\tau_{cr}$ of the PC specimen was compared with that from Equation (5). The experimental results showed general agreement with the calculated results from Equation (5).

Next, the joint strength was investigated for the specimens where joint failure occurred. The joint strength during the experiments was obtained from Equation (6). V_{jmax} is the maximum shear force input to the joint during the experiments. It is obtained using the same method as used for V_{jcr}. The joint shear strength was obtained from Equation (7).

$$_{ex}F_j = \frac{V_{jmax}}{\kappa \cdot \phi \cdot b_j \cdot D_j} \tag{6}$$

$$F_j = 0.8\sigma_B^{0.7} \tag{7}$$

[κ: Shape factor of joint ($\kappa = 1.0$), ϕ: Correction factor due to whether there are orthotropic beams or not ($\phi = 0.85$), σ_B: Compressive strength of concrete]

Experimental results complied with Equation (6) and F_j estimated from Equation (7) are shown in Figure 10. The experimental and calculated results were compared. RC55-50 showed agreement with Equation (7). However, the PC55-C-50 results were about 20% larger, exceeding the joint shear strength. The equation of joint strength where it is assumed that beam prestress force should bear part of shear strength input to the joint is defined by Equation (8).

$$_{PC}F_j = 0.8\sigma_B^{0.7} + \frac{\alpha \cdot P_{ini}}{\kappa \cdot \phi \cdot b_j \cdot D_j} \tag{8}$$

[α: Correction factor due to beam prestress, P_{ini}: Initial prestressing force]

Results obtained when $\alpha = 0.4$ in Equation (8) are shown with a dashed line in Figure 10. Good agreement was seen in the results obtained from Equation (8) and those of PC55-C-50 where the shear reinforcing bar at the joint reached yield. Only one PC specimen reached shear failure. The conditions of the damaged joint of the other PC specimens showed that the joint had larger strength than estimated from Equation (7). About a 40% Increase from the initial anchoring force was expected. Accumulation of further experimental data is necessary in the future.

4. MODELING OF ENVELOPE

The $Q - R$ relationship envelope for the frame using PC Mild Press Joint was modeled. It was assumed that the envelope moved to secondary rigidity during release of the initial press binding and it should become tri-linear when the rigidity became zero when the frame reached yield. The first inflection point in the envelope was shown to be at the intersection of the initial rigidity and the moment when release of press binding occurred. The initial rigidity was calculated taking into account only bending deformation, assuming the rigidity region specified in RC standard[2] in the beam/column joint at the cross-shaped part of the frame. The moment at press binding release (the first inflection point in the envelope) M_1 was calculated from Equation (9). This is the moment when a force equivalent to the initial force was applied to the tensile side of the prestressing strand. M_1 was converted to the story shear force Q_1.

$$M_1 = \Sigma T \cdot j = (E_p \cdot \varepsilon_{pt} \cdot A_{pt} + E_p \cdot \varepsilon_{pc} \cdot A_{pc}) \cdot j = (E_p \cdot \varepsilon_{pini} \cdot A_{pt} + E_p \cdot \varepsilon_{pc} \cdot A_{pc}) \cdot j \tag{9}$$

$$Q_1 = \frac{M_1}{a} \cdot \frac{L}{H} \tag{10}$$

[A_{pt}: Cross-sectional area of tensile side of prestressing strand, A_{pc}: Cross-sectional area of compression side of prestressing strand, E_p: Young's modulus of prestressing strand, ε_{pt}: Strain of tensile side of prestressing strand, ε_{pc}: Strain of compressive side of prestressing strand, j: Distance between tension and compression resultants, ε_{pini}: Initial strain of prestressing strand at the time of anchoring, a: Shear span, L: Beam span, H: Elevation between stories]

ε_{pc} was obtained by applying Popovics' Equation[3] for the stress - strain relationship of the concrete and from the cross-sectional analysis using Navier's hypothesis taking into account ε_{pini}. Next, the second inflection point in the envelope was obtained. It was assumed that the strain in the tensile side prestressing strand was the strain for 90% of the load against 0.2% permanent elongation in the tensile test for the prestressing strand. The moment M_2 at the second inflection point in the envelope was calculated by setting $\varepsilon_{pt} = \varepsilon_{pini} + \Delta\varepsilon_p = \varepsilon_{0.9}$ in Equation (9). Story drift angle at the second inflection point R_2 in the envelope was obtained from Equation (12) where the rotational angle of the press joint was obtained from Equation (11). It was judged that Equation (12) could be applied to the frames using the PC Mild Press Joints. This is because the deformation due to the rotational angle of the press joint occupied almost 100% of the story drift angle for the region larger than $R = 1/100$ rad. Also, δ_2 as an extracted quantity of prestressing strand was obtained from Equation (13)

$$\theta_2 = \frac{\delta_2}{\alpha} \tag{11}$$

$$R_2 = \frac{2(\theta_2 \cdot a)}{L} \tag{12}$$

$$\delta_2 = 2\int \varepsilon(x)dx = \Delta\varepsilon_p \cdot l_x \tag{13}$$

[α: Distance from the neutral axis to the tensile side prestressing strand, δ_2: Extract quantity of prestressing strand, $\Delta\varepsilon_p$: Incremental strain of prestressing strand on the beam column interface]

It was assumed that strain used for the extract quantity of prestressing strand δ_2 was in the symmetrical triangle distribution having a beam column interface at the center, as shown in the lower part of Figure 11. Results of the bond tests[4] carried out for the prestressing strands used in the experiments were reviewed for the strain distribution. The bond length l_x was defined by Equation (14).

$$l_x = \frac{\Delta\varepsilon_p \cdot E_p \cdot A_p}{\tau_{ave} \cdot \psi} \tag{14}$$

[τ_{ave} : $\tau_{ave} = 1.43$ N/mm^2 from the average bond stress of the prestressing strand and grout material (Bond test [4]), ψ : Periphery of prestressing strand surface (= 53.34 mm)]

Results obtained from the method employed in this study are shown by a bold solid line in Figure 12. As a result, it can be generally concluded that the method can model the envelope.
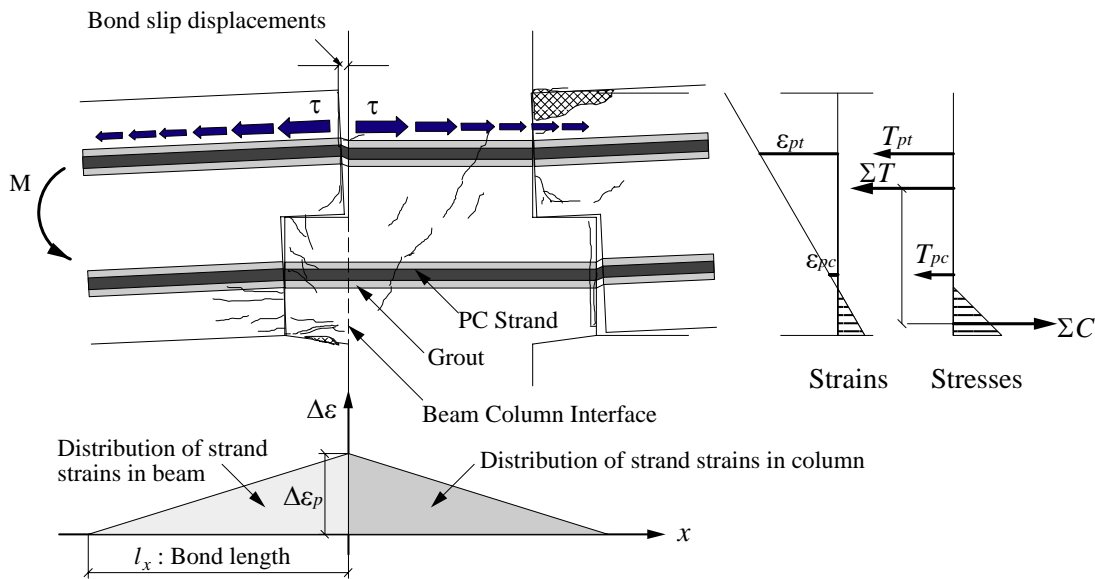

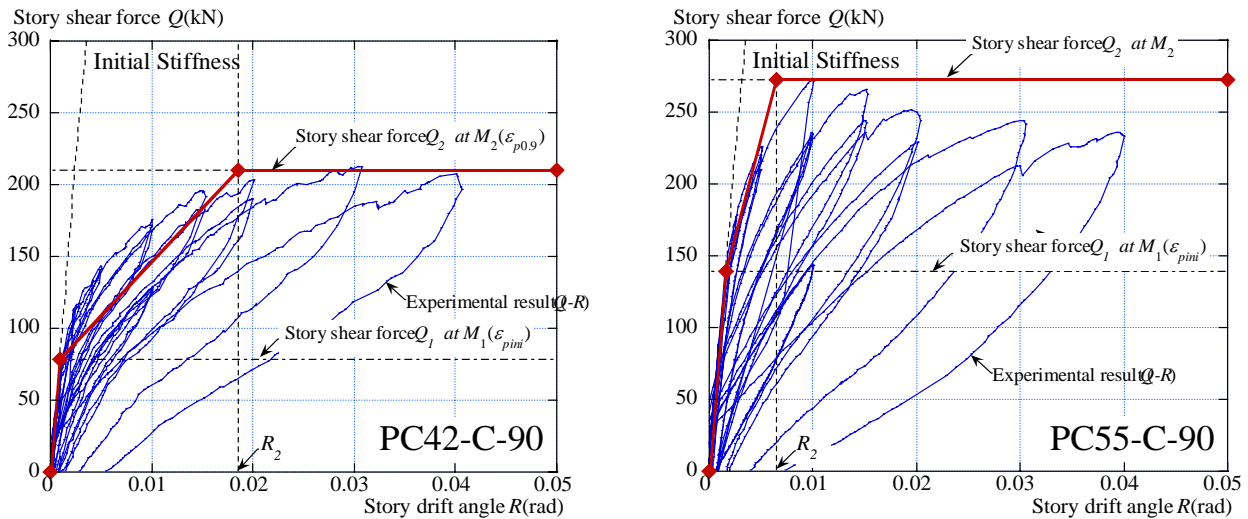Figure 11   Strains of PC Strands and Bond Slip Displacement

Figure 12   Experiment Results and Tri-Linear Envelope

5.   CONCLUSIONS

The following conclusions were drawn from the study where partial frame experiments were conducted using prestressing strands and verification was obtained by comparison with RC frames.

1) Hysteresis characteristics of the frame using the PC Mild Press Joint were noted. Extremely small residual deformation showed high restoration capability.
2) Damage was limited to the part near the beam column interface. Damage could be controlled.
3) Shear crack strength of the joint could be evaluated by taking into account the beam prestress.
4) Increase in shear strength of the joint by about 40% of the initial anchoring force can be expected for the current specimens.
5) Envelope of rigidity and strength of the frames with PC Mild Press joints could be modeled using the proposed method.

References:
1) Matsuzaki, Y., Wada, A. et. Al. (2001), "Damage Control Design by Precast-Prestressed Concrete Structure with MILD-PRESS-JOINT (Part1-Part4)", Summaries of Technical Papers of Annual Meeting Architectural Institute of Japan C-2, pp.893-900
2) Architectural Institute of Japan (1999), "All Standard for Structural Calculation of Reinforced Concrete Structures –Based on Allowable Stress Concept- revised 1999"
3) Popovics, S. (1973), "A Numerical Approach to The Complete Stress-Strain Curve of Concrete, *Cement and Concrete Research*, **3**, pp583—559
4) Matsuzaki, Y., Wada, A., Sakata, H. et. Al. (2003), "Study on Damage Control Design by Precast-Prestressed Concrete Structure with MILD-PRESS-JOINT (Part3. Bond Behavior) Summaries of Technical Papers of Annual Meeting Architectural Institute of Japan C-2, pp.991-992